Available online at www.sciencedirect.com

ScienceDirect

IFAC PapersOnLine 56-2 (2023) 5451–5456

Input and state constrained inverse optimal control with application to power networks ⋆

Taouba Kaouther Jouini * **Zhiyong Sun** ** **Venkatraman Renganathan** *** **Veit Hagenmeyer** *

* *Institute of Automation and Applied Informatics (IAI) at Karlsruhe Institute of Technology, Germany (e-mail: taouba.jouini@kit.edu, veit.hagenmeyer@kit.edu).*
** *Department of Electrical Engineering, Eindhoven University of Technology, Netherlands (e-mail: z.sun@tue.nl)*
*** *Department of Automatic Control, LTH, Lund University, Sweden (e-mail: venkatraman.renganathan@control.lth.se)*

Abstract: We study input and state constrained inverse optimal control problems starting from a stabilizing controller with a control Lyapunov function, where the goal is to make the controller an explicit solution of the resulting constrained optimal control problem. For an appropriate cost design and initial states for which a sublevel set of the Lyapunov function is contained in the state constraint set and the initial input lies on an ellipsoid inside the input constraint set, we show that the stabilizing controller solves the constrained optimal control problem. Compared to the state-of-the-art, we avoid solving nonlinear optimization problems evaluated pointwise, i.e., for every state, or in a repetitive fashion, i.e., at each time step. We apply our theoretical results to study the angular droop control studied in (Jouini et al., 2022) of an inverter-based power network. For this, we accommodate the constraints on the angle and power generation and exemplify our approach through a two-inverter case study.

Keywords: Optimal Control, Non-Linear Control Systems, Networked Systems, Power and Energy Systems

1. INTRODUCTION

Chronologically speaking, optimal control stems from the calculus of variation, a branch of mathematics dealing with path optimization in a static setting (Kot, 2014). The modern treatment of optimal control started from the late 1950s, when two mathematical breakthroughs were made (Vinter, 2010). First, the maximum principle gives a set of necessary conditions for a control solution candidate to be optimal (Liberzon, 2011). Second, dynamic programming provides necessary and sufficient conditions for optimality by solving the Hamilton-Jacobi-Bellman equation (Vinter, 2010). From an engineering point of view, many examples of optimal control problems arise spontaneously, every time a new quantity (e.g., product, accuracy of information) is synthesized while a performance index is taken into account.

In inverse optimal control (IOC), we start from a given stabilizing control law, with an associated control Lyapunov function and reverse engineer the cost function to render the stabilizing controller optimal. Thus, the control Lyapunov function is the value function of the resulting optimization problem as in (Haddad and Chellaboina, 2011; Sepulchre et al., 2012). In this way, we circumvent the complexity of solving partial differential equations. In fact, this approach provides analytically explicit and numerically feasible solutions in a simple, concise and closed form. Upon tuning of inverse optimal controllers, the solution to a whole family of optimal control problems corresponding to different cost functions is obtained with the *same* value function. We can solve inverse optimal control problems in the presence of unknown bounded disturbances in the dynamics as in (Freeman and Kokotovic, 1996) and also in the cost as illustrated in (Jouini and Rantzer, 2021). In applications to networked systems such as power networks, inverse optimal stabilizing controllers have a topological structure (e.g., distributed) and thus are feasible for implementation. In particular, an inverse optimal stabilizing controller for power networks is derived in (Jouini et al., 2022), namely the angular droop control. This control law stabilizes the phase angles of controllable voltage source inverters to an induced steady-state angle characterized by zero frequency error and thereby minimizes angle and power deviations at steady state.

Incorporating input and state constraints makes optimal control problems harder to solve. Inverse optimal control is an approach that solves optimal control problem with no computational effort by reverse engineering the cost. This motivates the study of inverse optimal control problems with input and state constraints. Despite recent efforts in the direction of incorporating given input (Nakamura et al., 2007) and state (Deniz et al., 2020) constraints

⋆ This work was supported by the Helmholtz Association under the program "Energy System Design".

10.1016/j.ifacol.2023.10.196

separately, inverse optimal control problems that account for both input and state constraints *simultaneously* as in (Freeman and Kokotovic, 1996) have not been extensively studied in the literature. More recent applications of inverse optimal problems have been pronounced at the interface of data-driven control and reinforcement learning via so-called *cost learning* (Finn et al., 2016). The aim in these works is to determine, for unknown dynamics and an observed solution of the optimal trajectories, the optimization criterion that has produced the solution. Recent research involves not only the learning of the cost but also the state and input constraints for constrained optimal control problems following (Menner et al., 2019).

In the present work, we consider an infinite horizon continuous-time input and state constrained inverse optimal control problem, i.e., the cost is determined after a stabilizing controller with a control Lyapunov function is specified. For this, we initialize the trajectory on a sublevel set of the Lyapunov function contained in the state constraint set and the input on a an ellipsoid lying inside of the input constraint set. In this way, we find upon suitable cost design an explicit solution to the constrained optimal control problem given by the controller that is simple, concise and has a closed-form expression. Compared to other methods that handle constraints in the inverse setting, where the cost is determined aposteriori, our approach does not require the computational effort of solving nonlinear programs pointwise, that is the case for pointwise minimum norm controllers (Freeman and Kokotovic, 1996). When the cost is given apriori as in Model Predictive Control (MPC) (Morari and Lee, 1999), we avoid repetitively solving an open loop optimization problem. Finally, inverter-based power networks are a direct application of our theory, where the constraints on the input norm represent lower and upper limits on the total power generation and constraints on the states consist in upper and lower bounds on the inverters' virtual angles.

The paper unfurls as follows. Section 2 presents the setup and in particular the inverse optimal control problem with input and state constraints. Section 3 proposes a solution approach and compares it with other approaches. Section 4 suggests a numerical implementation for a two-inverter power network. Finally, Section 5 concludes the paper.

Notation: For a continuously differentiable function $V : \mathbb{R}^n \to \mathbb{R}$, $\nabla_x V(x) = \frac{\partial V}{\partial x}$ denotes its gradient. Given a matrix $P = P^\top > 0$ and a vector v, we denote by $\|v\|_P = \sqrt{v^\top P v}$ the 2-norm of v weighted by P. Given a non-empty set $\mathcal{C}$, we denote by $\operatorname{int}\mathcal{C}$ the interior of $\mathcal{C}$.

2. PROBLEM FORMULATION

Consider the continuous-time input-affine system dynamics

$$\dot{x} = f(x) + G^\top(x)\, u(x), \quad x(0) = x_0\,, \tag{1}$$

where $f : \mathbb{R}^n \to \mathbb{R}^n$ is locally Lipschitz continuous over $\mathbb{R}^n$ with $f(0) = 0$, and the input matrix $G(x) = [g_1^\top(x), \ldots, g_m^\top(x)]^\top \in \mathbb{R}^{m\times n}$ is given by the nonlinear functions $g_i(x)$, $i = 1, \ldots m$ that are continuous mappings from $\mathbb{R}^n$ to $\mathbb{R}^n$. The state and input vectors are given by $x \in \mathbb{R}^n$ and $u \in \mathbb{R}^m$. Furthermore, let the following infinite horizon continuous-time optimal control problem be given,

$$\underset{u\in\mathcal{U}}{\text{minimize}} \quad \int_0^\infty \left[q(x) + u^\top(s)R(x)\,u(s) + \delta^\top(x)u(s)\right] \mathrm{d}s \tag{2a}$$

$$\text{subject to} \quad \dot{x} = f(x) + G^\top(x)\,u, \tag{2b}$$

$$x(0) = x_0,\, x \in \mathcal{X}, \tag{2c}$$

where $\mathcal{U} \subset \mathbb{R}^m$ and $\mathcal{X} \subset \mathbb{R}^n$ are given input and state constraint sets. Additionally, the function $q : \mathbb{R}^n \to \mathbb{R}$ is continuous with $q(0) = 0$ and assumed to be unknown and $R(x) = R^\top(x) > 0$ for all x. Here $\delta : \mathbb{R}^n \mapsto \mathbb{R}^m$ is a weighting function satisfying $\delta(0) = 0$. Notice that the function δ provides flexibility in the cost design that can be exploited for instance to connect inverse optimal control with backstepping methods as shown in (Haddad and Chellaboina, 2011, Ch.9).

Our goal in the remainder is to solve the constrained optimal control problem (2) based on inverse optimality by determining the cost function as in (Sepulchre et al., 2012; Freeman and Kokotovic, 1996; Haddad and Chellaboina, 2011; Jouini and Rantzer, 2021).

3. SOLUTION APPROACH AND DISCUSSION

3.1 Solution approach

We start from the following feedback control law

$$u^f(x) = -\frac{1}{2}\, R^{-1}(x)\Big(G(x)\nabla_x V(x) + \delta(x)\Big), \tag{3}$$

together with a continuously differentiable function $V : \mathbb{R}^n \to \mathbb{R}_+$ with $V(0) = 0$ satisfying,

$$\nabla_x^\top V(x)(f(x) + G^\top(x)u^f(x)) < 0. \tag{4}$$

In the remainder, the input and state constraint sets $\mathcal{U}$ and $\mathcal{X}$ are given by the following assumption.

Assumption 1. *We assume that $\mathcal{U}$ and $\mathcal{X}$ are closed. Additionally, let $0 \in int(\mathcal{X})$ and $0 \in int(\mathcal{U})$. For $M(x) = M^\top(x) > 0$, let*

$$\mathcal{C}_\gamma := \{u \in \mathbb{R}^m \mid \|u\|_{M(x)} \le \gamma\} \subseteq \mathcal{U}, \tag{5}$$

where γ is a positive constant.

Sufficient conditions for the controller $u^f(x)$ in (3) to solve the constrained inverse optimal control problem (2) are specified in the following theorem.

Theorem 3.1. *Let Assumption 1 hold. For a given constant $c > 0$, consider*

$$\Omega_c = \{x \in \mathcal{X} \mid V(x) \le c\}, \tag{6}$$

such that $\Omega_c \subseteq \mathcal{X}$. For $x_0 \in \Omega_c$ and $u^f(x_0) \in \mathcal{C}_\gamma$, let

$$q(x) = -\nabla_x^\top V(x)f(x) + u^{f\top}(x)\, R(x)\, u^f(x), \tag{7}$$

then, the controller $u^f(x)$ in (3) minimizes (2). Additionally, the optimal control problem (2) has the optimal value $V(x_0)$.

Proof. We apply Theorem 8.2 in (Haddad and Chellaboina, 2011) as follows. First, we show that $u^f(x) \in \mathcal{U}$ by showing that $u^f(x) \in \mathcal{C}_\gamma$ if $u^f(x_0) \in \mathcal{C}_\gamma$.

Following (4), the set Ω_c is control invariant under the action of $u^f(x)$ (Blanchini, 1999) and is thus a forward invariant set, i.e., $x(t) \in \Omega_c \subseteq \mathcal{X}$ given that $x_0 \in \Omega_c$ for all future times $t > 0$. Since the origin is a minimum of V and $\delta(0) = 0$, the (scaled) magnitude of $u^f(x)$ is decreasing as the closed-loop trajectory approaches the origin starting from $x_0 \in \Omega_c$, i.e., $\|u^f(x)\|_{M(x)} \leq \|u^f(x_0)\|_{M(x_0)}$ holds.

Combining the above inference with $u^f(x_0) \in \mathcal{C}_\gamma$, we have $\|u^f(x)\|_{M(x)} \leq \gamma$. This shows that $u^f(x) \in \mathcal{C}_\gamma$. From $\mathcal{C}_\gamma \subseteq \mathcal{U}$, it follows that $u^f(x) \in \mathcal{U}$.

Second, we define $L(x,u) = q(x)+u^\top R(x)\, u+\delta^\top(x)u$ with q as in (7) and show that the Hamilton function satisfies

$$H(x,u) = L(x,u) + \nabla_x^\top V(x)(f(x) + G^\top(x)u) \geq 0.$$

For the feedback controller $u^f(x)$ in (3), our calculations show that

$$\begin{aligned} H(x,u^f(x)) &= L(x,u^f(x)) + \nabla_x^\top V(x)(f(x) + G^\top(x)u^f(x)) \\ &= 0. \end{aligned}$$

Since the function H is convex in u, the first order condition $\frac{\partial H}{\partial u} = 0$ is necessary and sufficient for a minimum. This corresponds to $u(x) = u^f(x)$. Therefore $H(x,u) \geq H(x,u^f(x)) = 0$ and $u^f(x)$ satisfies all the conditions of Theorem 8.9 of (Haddad and Chellaboina, 2011) with the Lyapunov function V in (4). This shows that the feedback controller $u^f(x) \in \mathcal{U}$ in (3) minimizes (2) and the optimal value is $V(x_0)$. □

A direct consequence of Theorem 3.1 is given in the following Corollary.

Corollary 3.2. *Let Assumption 1 hold and consider the optimization problem (2) with $\delta(x) = 0$ given by*

$$\underset{u\in\mathcal{U}}{\text{minimize}} \quad \int_0^\infty \left[q(x) + u^\top(s)R(x)\,u(s)\right] \mathrm{d}s \tag{8a}$$

$$\text{subject to} \quad \dot{x} = f(x) + G^\top(x)\,u, \tag{8b}$$

$$x(0) = x_0,\ x \in \mathcal{X}. \tag{8c}$$

Consider the feedback controller,

$$\tilde{u}^f(x) = -\frac{1}{2}\,R^{-1}(x)G(x(k))\nabla_x\tilde{V}(x), \tag{9}$$

and a continuously differentiable function $\tilde{V} : \mathbb{R}^n \to \mathbb{R}_+$ with $\tilde{V}(0) = 0$ satisfying,

$$\nabla_x^\top\tilde{V}(x)(f(x) + G^\top(x)\tilde{u}^f(x)) < 0. \tag{10}$$

Furthermore, let Ω_c and $\mathcal{C}_\gamma$ as in (6) and (5) with $\Omega_c \subseteq \mathcal{X}$ and $\mathcal{C}_\gamma \subseteq \mathcal{U}$. Given $x_0 \in \Omega_c$ and $\tilde{u}^f(x_0) \in \mathcal{C}_\gamma$, suppose that

$$q(x) = -\nabla_x^\top\tilde{V}(x)f(x) + \tilde{u}^{f\top}(x)\,R(x)\,\tilde{u}^f(x). \tag{11}$$

Then, $\tilde{u}^f(x)$ in (9) minimizes (8). Additionally, the optimal control problem (8) has the optimal value $\tilde{V}(x_0)$.

3.2 Discussion

- Selecting the positive constants $c, \gamma > 0$ in (6) and (5), respectively, can be cast as optimization programs. In the first problem, we find the largest sublevel set of V by maximizing c such that $\Omega_c \subseteq \mathcal{X}$. In the second program, we determine the largest set $\mathcal{C}_\gamma \subseteq \mathcal{U}$ by maximizing γ. By choosing the parametrization $c = V(x_0)$ and $\gamma = u^f(x_0)$ these two programs are merged into one that solves for the initial condition x_0.
- For $\delta(x) = 0$, we note the results on inverse optimality of input-affine systems found in (Haddad and Chellaboina, 2011) are a relaxed version of our approach in (Jouini and Rantzer, 2021) by selecting a Lyapunov function, whose derivative along closed-loop trajectories is negative (and not upper bounded by a negative definite function) and a cost functional that is real-valued (and not positive definite)

3.3 Result contextualization

In the light of Theorem 3.1 and Corollary 3.2, we compare our approach to the state-of-the-art literature in solving constrained optimal control problems for the direct formulation, i.e., where the cost is known and given as in Model Predictive Control, as well as the inverse setting of the pointwise min-norm controller, where the cost is determined *a posteriori*.

Model Predictive Control (MPC) If we consider the discrete-time version of the optimal control problem (2) and a given cost function, MPC approach finds an open-loop control sequence over a horizon length N by evaluating the state trajectories starting from an initial state $x(0)$, where only the first element in the input sequence is applied. It is a repetitive decision making process, i.e., that solves an open-loop optimization problem at each time step and has the inherent ability to systematically handle input and state constraints (Goebel and Raković, 2019).

Pointwise min-norm controller The input and state constrained inverse optimal control problem (2) has been solved in (Freeman and Kokotovic, 1996) by suggesting the pointwise minimum norm controller. Freeman and Kokotovic proposed to solve a convex program to find the pointwise min-norm controller that includes solving a static nonlinear program. The pointwise min-norm controller finds for every x, the controller u with minimum (possibly scaled) norm $\|u(x)\|_{H(x)}$ with $H(x) > 0$ that satisfies the input constraints. Following the Control Barrier Function (CBF) formulation in (Ames et al., 2016), the quadratic program of finding the min-norm controller can be augmented with an inequality for a control barrier function to additionally account for state constraints.

Compared to these methods, our approach provides a closed-form solution to the constrained inverse optimal control problem (2) without resorting to solving optimization problems in a repetitive (as in MPC) or pointwise fashion (i.e., for pointwise min-norm controller, also incremented with CBF).

4. APPLICATION TO POWER SYSTEM NETWORKS

In this section, we study a constrained optimal control problem arising in angle control of inverter-based power networks. The goal is to stabilize the inverter angles at an induced steady-state angle while keeping the angle deviations and input effort within prescribed bounds. In particular, we consider a connected undirected graph, where the set of nodes consists of $n-$phase coupled oscillators, representing controllable voltage sources (with constant voltage magnitude, i.e., 1 per unit), whose angle (relative to an angle rotating at nominal frequency ω^*) dynamics are described by the following first-order integrator dynamics,

$$\dot{\theta} = u, \quad \theta(0) = \theta_0, \tag{12}$$

where $\theta = [\theta_1, \dots, \theta_n]^\top \in \mathbb{R}^n$ is the angle vector. The set of edges consists of inductive (i.e., lossless) $m-$transmission lines. The coupling strengths are represented by line susceptance $b_{ij} > 0$ for $j \in \mathcal{N}_i$, where $\mathcal{N}_i$ denotes the neighborhood set of the $i-$th inverter node. An example network of two inverters is represented in Fig. 1.

The active power deviation from the nominal value is given by,

$$P_i(\theta) - P_i^* = \sum_{j \in \mathcal{N}_i} b_{ij} \left(\sin(\theta_{ij}) - \sin(\theta_{ij}^*)\right),$$

where $\theta_{ij} = \theta_i - \theta_j$ and $\theta_{ij}^* = \theta_i^* - \theta_j^*$. Here $\{\theta_i^*\}_{i=1}^n$ are the nominal steady state angles, $P_i(\theta)$ is its active power injected into the network and P_i^* is its nominal active power.

Let $\theta^s := \lim_{t\to\infty} \theta(t)$ be an induced steady state angle of (12) satisfying

$$\xi\left(\theta^s - \theta^*\right) = P^* - P(\theta^s), \tag{13}$$

with $\xi > 0$ is the angle to power droop gain. By taking the time derivative of (13), we show in (Jouini et al., 2022) that θ^s rotates at the nominal frequency ω^*. Notice that when there is no power imbalance, i.e., $P^* - P(\theta^s) = 0$, the induced steady state angle corresponds to the nominal steady state angle, i.e., $\theta^s = \theta^*$.

We make the following assumption stating that neighboring steady state angle differences are contained in an arc of length π.

Assumption 2 ((Jouini et al., 2022)). *The induced steady state angle $\theta^s = \{\theta_k^s\}_{k=1}^n$ satisfies $\mathcal{B}^\top \theta^s \in \left(-\frac{\pi}{2}, \frac{\pi}{2}\right)^m$, where $\mathcal{B} \in \mathbb{R}^{n\times m}$ is the incidence matrix of the underlying graph.*

Next, let $R = R^\top > 0$ be the input penalty matrix and consider the following optimal control problem,

$$\begin{aligned} \underset{u\in\mathcal{U}}{\text{minimize}} \quad & \int_0^\infty q(\theta(s)) + \|u(s)\|_R^2 \mathrm{d}s \\ \text{subject to} \quad & \dot{\theta} = u,\ \theta(0) = \theta_0, \\ & \theta \in \mathcal{X} \end{aligned}$$

Here $q : \mathbb{R}^n \to \mathbb{R}$ with $q(\theta^s) = 0$ is a function that will be determined in the sequel and $\theta_0 \in \mathcal{X}$. The constraints on the state are represented by the following set

$$\mathcal{X} := \{\theta \in \mathbb{R}^n | \quad \underline{\theta} - \theta^s \le \theta - \theta^s \le \overline{\theta} - \theta^s\}, \tag{15}$$

with $\underline{\theta} \le \theta^s$ and $\theta^s \le \overline{\theta}$ are upper and lower limits on the admissible inverter angles and therefore $\theta^s \in \mathcal{X}$. These can be obtained for instance from minimal and maximal electrical power output at each inverter $\underline{P} \le P(\theta) \le \overline{P}$ with $P(\theta) = [P_1(\theta), \dots, P_n(\theta)]^\top$ and $\underline{P}, \overline{P} \in \mathbb{R}^n$ are the vectors of minimum and maximum power output. The input is constrained by the overall power generation limit and given by

$$\mathcal{U} := \{u \in \mathbb{R}^n : \|u\|_M \le \gamma\}, \tag{16}$$

with $\gamma > 0$ and $M = M^\top > 0$. Let $\Xi = \xi I_n$ and define the following function

$$V(\theta) = \frac{1}{2}\|\theta - \theta^s\|_\Xi^2 + \sum_{i=1}^n \sum_{j\in\mathcal{N}_i} b_{ij}\left(\cos(\theta_{ij}) - \cos(\theta_{ij}^s) - (\theta_{ij} - \theta_{ij}^s)\sin(\theta_{ij}^s)\right). \tag{17}$$

For $\epsilon > 0$, let $B_\epsilon(\theta^s) = \{\theta \in \mathbb{R}^n | \|\theta - \theta^s\| < \epsilon\}$ be a neighborhood of θ^s. Under Assumption 2, we show in (Jouini et al., 2022) that $V(\theta)$ in (17) is locally (i.e, in the neighborhood $B_\epsilon(\theta^s)$) positive definite.

Our approach based on inverse optimality following (Haddad and Chellaboina, 2011) and Corollary 3.2 suggests the choice of the cost function,

$$q(\theta) = \frac{1}{4}\Big(\Xi(\theta - \theta^*) + P(\theta) - P^*\Big)R^{-1}(\theta) \Big(\Xi(\theta - \theta^*) + P(\theta) - P^*\Big), \tag{18}$$

where,

$$\nabla_\theta V(\theta) = \Xi(\theta-\theta^s) + P(\theta) - P(\theta^s) = \Xi(\theta-\theta^*) + P(\theta) - P^*$$

with $P(\theta) - P^* = [P_1(\theta) - P_1^*, \dots, P_n(\theta) - P_n^*]^\top$ yields the locally inverse optimal stabilizing controller,

$$u^*(\theta) = -\frac{1}{2}R^{-1}\Big(\Xi(\theta - \theta^*) + P(\theta) - P^*\Big). \tag{19}$$

The angular droop controller in (Jouini et al., 2022) is given by (19).

Following Corollary 3.2, we numerically demonstrate in the following two-inverter network example depicted in Fig. 1 that for a chosen initial condition, the angle and input satisfy the constraints defined in (15) and (16). Table 4 summarizes the numerical values (in p.u.) of the case study.

Given $\gamma = 1$, we select $\theta_0 \in \mathcal{X}$ such that $c = V(\theta_0)$ and $\Omega_c \subseteq \mathcal{X}$ together with $\|u(\theta_0)\|_M \le 1$. The matrix M plays the role of virtual inertia and its value is taken from (Menta et al., 2018). By graphical inspection of Fig. 4, we find $\theta_0 = [2.5, -2]^\top \in \mathcal{X}$ and the sublevel $c = 6.7430$. In Fig. 2, the angle trajectories remain inside of the set $\mathcal{X}$ for all times t and the induced steady state $\theta^s = [0.5, -0.5]^\top$ satisfies Assumption 2. In Fig. 3, the scaled 2-norm of the input satisfies the constraints described in (16), where the cost in (18) and the input (19) are a decreasing function of time.

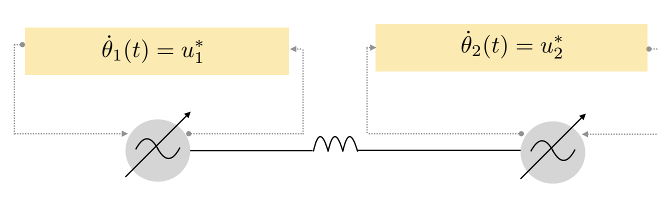

Fig. 1. Two-inverter system in closed-loop with angular droop (19).

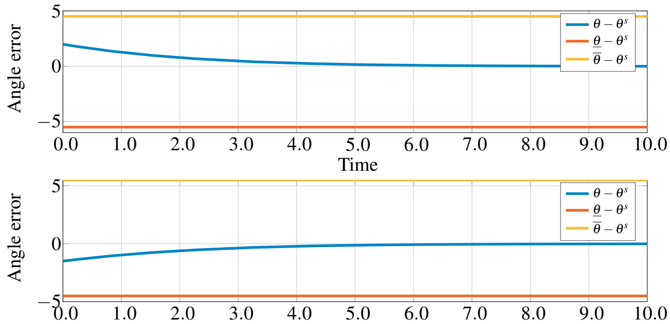

Fig. 2. Time-domain simulation of the angle error $\theta - \theta^s$ starting from $\theta_0 = [2.5, -2]^\top \in \mathcal{X}$ together with the minimum and maximum admissible angle deviations.

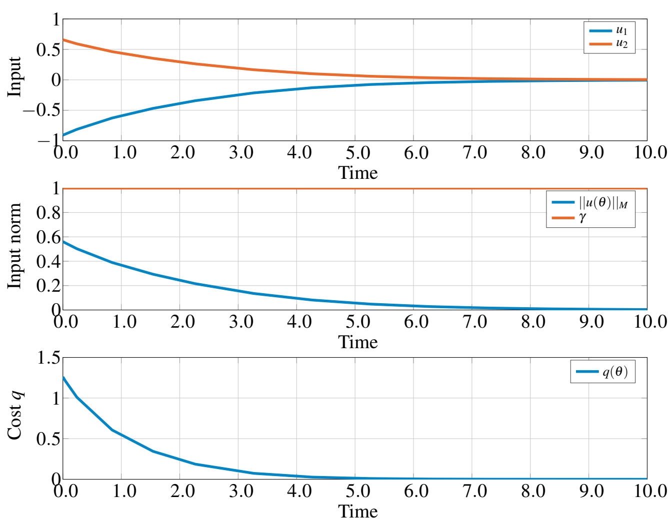

Fig. 3. Time-domain simulations of the inputs u as well as its norm in (16) for $\gamma = 1$. The cost $q(\theta)$ in (18) is decreasing function of the closed-loop angle trajectory.

5. CONCLUSION

We solved the constrained inverse optimal control problem for an input constraint set containing an ellipsoid and a state constraint set containing a sublevel set of the control Lyapunov function. Our future work aims to study the effect of choosing different Lyapunov functions to satisfy the state constraints and a numerical comparison with state-of-the-art methods from constrained optimization.

ACKNOWLEDGEMENTS

The first author would like to thank Anders Hansson for the insightful comments and suggestions.

Table 1. Parameter values in (p.u.)

Parameter	Value (in p.u.)
R	I_3
γ	1
M	$0.25 \cdot I_3$
ξ	1
b_{12}, b_{21}	0.1
c	6.7430
$\underline{\theta}$	$-5 \cdot [1, 1]^\top$
$\overline{\theta}$	$5 \cdot [1, 1]^\top$

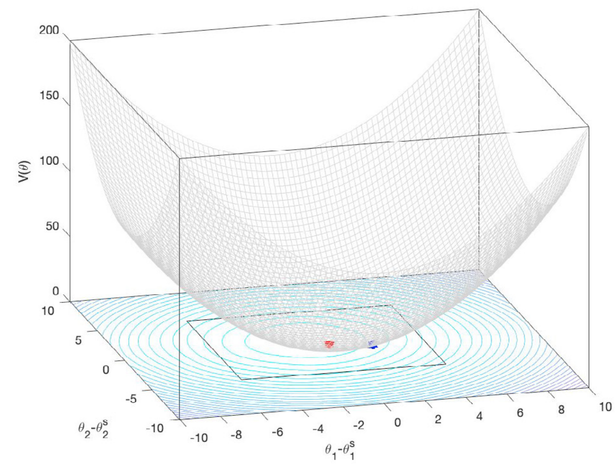

Fig. 4. 3-D Representation of the sublevel set of the Lyapunov function V in (17) in blue and the state constraint set $\mathcal{X}$ in (15) in black containing the origin marked by the red star. The initial condition $\theta_0 \in \mathcal{X}$ marked by the blue star is chosen such that the set Ω_c in (6) is contained in the box $\mathcal{X}$.

REFERENCES

Ames, A.D., Xu, X., Grizzle, J.W., and Tabuada, P. (2016). Control barrier function based quadratic programs for safety critical systems. *IEEE Transactions on Automatic Control*, 62(8), 3861–3876.

Blanchini, F. (1999). Set invariance in control. *Automatica*, 35(11), 1747–1767.

Deniz, M., Devi, P., and Balakrishnan, S.N. (2020). Inverse optimal control with set-theoretic barrier Lyapunov function for handling state constraints. In *2020 American Control Conference (ACC)*, 981–986. doi: 10.23919/ACC45564.2020.9147707.

Finn, C., Levine, S., and Abbeel, P. (2016). Guided cost learning: Deep inverse optimal control via policy optimization. In *International conference on machine learning*, 49–58. PMLR.

Freeman, R.A. and Kokotovic, P.V. (1996). Inverse optimality in robust stabilization. *SIAM Journal on Control and Optimization*, 34(4), 1365–1391.

Goebel, R. and Raković, S.V. (2019). Set-valued and Lyapunov methods for MPC. In *Handbook of Model Predictive Control*, 53–73. Springer.

Haddad, W.M. and Chellaboina, V. (2011). *Nonlinear dynamical systems and control*. Princeton University Press, Princeton, New Jersey.

Jouini, T. and Rantzer, A. (2021). On cost design in applications of optimal control. *IEEE Control Systems Letters*, 6, 452–457.

Jouini, T., Rantzer, A., and Tegling, E. (2022). Inverse optimal control for angle stabilization in converter-based generation. In *2022 American Control Conference (ACC)*, 4945–4950. doi: 10.23919/ACC53348.2022.9867726.

Kot, M. (2014). *A first course in the calculus of variations*, volume 72. American Mathematical Society.

Liberzon, D. (2011). *Calculus of variations and optimal control theory: a concise introduction*. Princeton university press.

Menner, M., Worsnop, P., and Zeilinger, M.N. (2019). Constrained inverse optimal control with application to a human manipulation task. *IEEE Transactions on Control Systems Technology*, 29(2), 826–834.

Menta, S., Hauswirth, A., Bolognani, S., Hug, G., and Dörfler, F. (2018). Stability of dynamic feedback optimization with applications to power systems. In *2018 56th Annual Allerton Conference on Communication, Control, and Computing (Allerton)*, 136–143. doi: 10.1109/ALLERTON.2018.8635640.

Morari, M. and Lee, J.H. (1999). Model predictive control: past, present and future. *Computers & Chemical Engineering*, 23(4-5), 667–682. doi:10.1016/S0098-1354(98)00301-9.

Nakamura, N., Nakamura, H., Yamashita, Y., and Nishitani, H. (2007). Inverse optimal control for nonlinear systems with input constraints. In *2007 European Control Conference (ECC)*, 5376–5382. doi: 10.23919/ECC.2007.7068412.

Sepulchre, R., Jankovic, M., and Kokotovic, P.V. (2012). *Constructive nonlinear control*. Springer Science & Business Media.

Vinter, R. (2010). *Optimal control*. Springer Science & Business Media, Berlin/Heidelberg, Germany.